Soft Matter

Cite this: *Soft Matter*, 2012, **8**, 4494

www.rsc.org/softmatter

PAPER

Morphological transformation between three-dimensional gel network and spherical vesicles *via* sonication†,‡

Mingming Zhang, Luyan Meng, Xinhua Cao, Meijuan Jiang and Tao Yi*

Received 21st January 2012, Accepted 20th February 2012
DOI: 10.1039/c2sm25164g

A novel low weight molecular gelator was designed and synthesized which can gelate several polar solvents with different morphologies. It is interesting that it exchanges morphology between a three-dimensional gel network and vesicles in ethanol *via* treatment with ultrasound and a heating-cooling process, through supramolecular self-assembly in a certain concentration range. The mechanism of the self-assembly process was investigated by IR, X-ray diffraction and rheological experiments. The results show that the gelator molecules self-assemble in a parallel manner into a lamella structure and the lamellas further aggregate into a gel network or vesicles at room temperature with or without the ultrasonic stimulation.

Introduction

As an important research topic in chemistry, self-assembly is not only disclosing the mystery of the origin of the life, but also directs the novel nanostructure of future materials.[1] One of the main challenges is to manipulate self-assembly of designed building blocks to formulate novel nanostructured materials that have the capability to be stimulus-responsive.[2] Vesicles, as a kind of typical self-assembly structure, have been extensively studied during the past decades for their potential applications, such as drug delivery,[3] templates for processing well-defined materials, biomaterials and food processing.[4] As we already know, most of these vesicles are made by amphiphilic polymers, surfactants and lipids through self-organization.[5] Recently, vesicles composed of low weight molecules (LWM) bonded through noncovalent interactions have also attracted attention.[6–8] The particular importance is the dynamic character of these LWM vesicles since their structure and functionality may be tuned by an outside stimulus and thus show advantages in biomedical applications and smart materials.

Ultrasound as one of the external stimulations has begun to play a significant role in the self-assembly of LWMs.[9,10] Sijbesma and Naota reported rheology switching and conformational changes in response to sonication, which induced supramolecular self-assembly leading to gelation of the liquid.[11] In our previous work, we used a classic linear aromatic-linked-sterol system by using a small peptide as a linker for fabricating different kinds of nano/microstructures including spheres, fibers and core-shells, which could respond to ultrasound in the gel state.[12] It was also interesting to observe that in cases of sonication-induced gelation, the critical gelation concentration is very different between the gel formed by a thermal process and that formed in response to sonication.[13] However, the synergistic effect of the concentration and sonication in the self-assembly process was not paid enough attention in previous studies. In this work, we propose an approach to achieve a reversible conversion between vesicles and a three dimensional gel network by means of self-assembly in response to heating and sonication in a certain concentration range.

Experimental section

General method

All of the starting materials were obtained from commercial suppliers and used as received. Moisture sensitive reactions were performed under an atmosphere of dry argon. Amantadine hydrochloride (99%) and cholesteryl choroformate (99%) were provided by Alfa Aesar; other chemicals were supplied from Sinopharm Chemical Reagent Co., Ltd. (Shanghai). Column chromatography was carried out on silica gel (200–300 mesh). ^{1}H-NMR (400 MHz) and ^{13}C-NMR (100 MHz) were recorded on a Mercuryplus-Varian instrument. Proton chemical shifts are reported in parts per million downfield from tetramethylsilane (TMS). MALDI-TOF-MS was recorded on BIFLEX III MALDI-TOF mass spectroscopy instrument (Bruker Daltonics Inc.). Melting points were determined on a hot-plate melting point apparatus XT4-100A without correction.

Department of Chemistry & Laboratory of Advanced Materials, Fudan University, 220 Handan Road, Shanghai, China. E-mail: yitao@fudan.edu.cn; Fax: +86 21 55664621; Tel: +86 21 55664330

† Electronic supplementary information (ESI) available: details of synthesis, supplementary images and spectral data. See DOI: 10.1039/c2sm25164g

‡ Dedicated to Professor Chunhui Huang for the occasion of her 80th birthday

Techniques

SEM images were obtained with the help of a FE-SEM S-4800 (Hitachi) instrument. Samples were prepared by spinning the samples on glass slices and coating with Au. TEM was performed on a JEOL JEM2011 apparatus operating at 200 kV. The samples were prepared by coating the diluted wet gels on a copper grid at room temperature and freeze drying (EYELA, FDU-1200) for 24 h. XRD diagrams were obtained on a D8 ADVANCE and DAVINCI.DESIGN (Bruker), using a Cu-Kα radiation source ($\lambda = 0.1542$ nm). Rheology experiments were performed on a MCR 301 Anton Paar rheometer (Austria), with a Couette cell and a temperature control unit. The measurements were carried out on freshly prepared gels by using a controlled-stress rheometer. Parallel plate geometry of 25 mm diameter and 1 mm gap were employed throughout the dynamic oscillatory tests. The following tests were performed: increasing amplitude of oscillation up to 100% apparent strain shear (kept at a frequency of 6.28 rad s^{-1}) and frequency sweeps at 20 °C (from 100–0.1 rad s^{-1}, 0.1% strain). Nitrogen adsorption–desorption isotherms were measured at −196 °C by using a Micromeritics ASAP Tristar 3000 system. The samples were degassed at 110 °C overnight on a vacuum line. The Brumauer–Emmett–Teller (BET) method was utilized to calculate the specific surface areas. Time-resolved FTIR spectra were collected by an *in situ* ReactIR 45m (Mettler Toledo) spectrometer equipped with a silicon probe and a resolution of 8 cm^{-1} was available for an acceptable signal-to-noise ratio. Powder IR spectra were collected by a Nexus 470 spectrometer (Nicolet Company) with a resolution of 4 cm^{-1}, and 64 scans were accumulated to obtain an acceptable S/N ratio, the samples were prepared with KBr pellets.

Gelation test of organic fluids

The gelators and solvents were put in a septum-capped test tube and heated (50–85 °C) until the solid dissolved. Then the sample vial was cooled to room temperature (prepared sample). If the prepared sample can form a gel when left for a period of time in a certain solvent (for example 10 min) at ambient conditions, it was denoted a T-gel. The gel which was obtained when the prepared sample treated by ultrasound (0.31 W cm^{-2}, 40 KHz) for 10 min at 25 °C was called an S-gel. Qualitatively, gelation was considered successful if no sample flow was observed upon inverting the container at room temperature (*i.e.*, the "inverse flow" method).

Results and discussion

The morphology of the self-assemblies

Building on our earlier work,[14] we designed a gelator with hydrophobic groups (an adamantane, a cholesteryl group) at both ends of the molecule, linked by a hydrophilic amide chain (compound **1** in Scheme 1). The hydrogen bonds of the amide groups and the hydrophobic interactions of the cholesteryl group are responsible for the orientation and orderly arrangement of the gelator molecules. Therefore, compound **1** can gelate a variety of polar solvents, including ethanol, DMF, DMSO and isopropanol, within a certain range of concentrations (Table S1, see ESI†).

The morphology of the aggregation represents the result of the self-assembly process at the macro level, which is very sensitive to

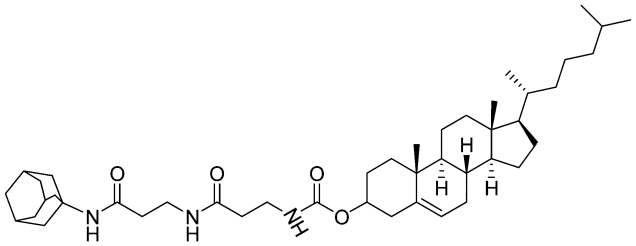

Scheme 1 Structure of compound **1**.

the conditions. Here, we found that the morphology of the self-assemblies of **1** was quite different with the solvent from the scanning electron microscopy images (SEM, Fig. 1). A large area of honeycomb-like sheet structures with a thickness about 50 nm was observed in the gel sample of **1** in DMSO at a concentration of 4.3 wt% (Fig. 1a). The SEM image of the gel in DMF showed a large amount of ribbons with a length of about 10 μm and breadth of about 70 nm (5.0 wt%, Fig. 1b). While in isopropanol, the gel gives a ribbon structure with a length of about 2–10 μm and breadth of about 500 nm (6.0 wt%, Fig. 1c). An SEM image of a precipitate sample of **1** from methanol at a concentration of 1.8 wt% was also measured and showed a large number of squashed ball structures with diameters in the range of 400–600 nm (Fig. 1d).

It is interesting that the gel formation in ethanol depends on the concentration and sonication irradiation. For example, **1** could not gelate ethanol by a heating–cooling process at a concentration lower than 4.4 wt%. In the range of 0.44–4.4 wt %, **1** behaves as a sol at a higher temperature (>50 °C), but as a flocculent precipitate at room temperature (25 °C). The self-assembly character of the precipitate of **1** at different concentrations of 1.2 wt%, 2.4 wt% and 3.5 wt% in ethanol after the heating–cooling process was studied by SEM images. It is surprising that SEM images of all the precipitate samples with the concentration range from 1.2–3.5 wt% showed globular structures with the diameter slightly decreasing with the increase

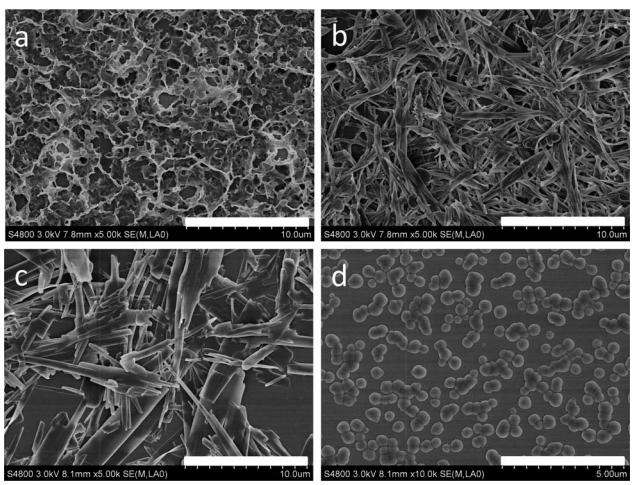

Fig. 1 SEM images of compound **1** in different solvents from a heating–cooling process: (a) gel in DMSO (4.3 wt%), (b) gel in DMF (5.0 wt%), (c) gel in isopropanol (6.0 wt%), (d) precipitate in methanol (1.8 wt%), scale bar for a, b and c is 10 μm, for d it is 5 μm.

of concentration (Fig. 2a and Fig. S1, see ESI†). This may be due to the increase in the supersaturation of the gelator, which increases the nucleation rate.[15] Transmission electron microscopy (TEM) revealed that the globular structure was a hollow vesicle with the thickness of the vesicle at around 2.8 nm (Fig. 2c and 2d). However, a T-gel was formed after a heating–cooling process at a concentration larger than 4.4 wt% (gel formation concentration, CGC). The SEM image of a gel sample at 4.6 wt% showed a large amount of ribbon with a length of about 5–10 μm and breadth of about 200–300 nm (Fig. 2b).

After being treated with sonication in ethanol for 10 min (500 w, 40 KHz), the gel could also be formed; however, the CGC is reduced to 1.7 wt% with sonication. For example, when 10 mg of **1** was added to 0.5 mL of ethanol, the mixture was changed into a transparent sol when heated at 70 °C for 15 min. The transparent sol was completely changed into a white gel after sonication for at least 10 min, and the gel remained non-flowing for 1 month (Fig. 3). The gel was changed into a transparent sol again by heating at 70 °C for 24 s. Therefore, we could use this special property to change the ethanol sol of **1** into a gel state or vesicles in the concentration range 1.7–4.4 wt% by sonication or by the heating–cooling process. Both the gel and vesicles can be returned to a sol by heating at 40–68 °C (gel to sol transition temperature, T_g, Fig. S2, see ESI†).

Our earlier work showed that sonication has some influence on the aggregation of molecules, resulting in a changed morphology.[12,13] Here, to understand the morphological changes of **1** between the heating–cooling and sonication treatment, samples under different conditions were observed by SEM. A

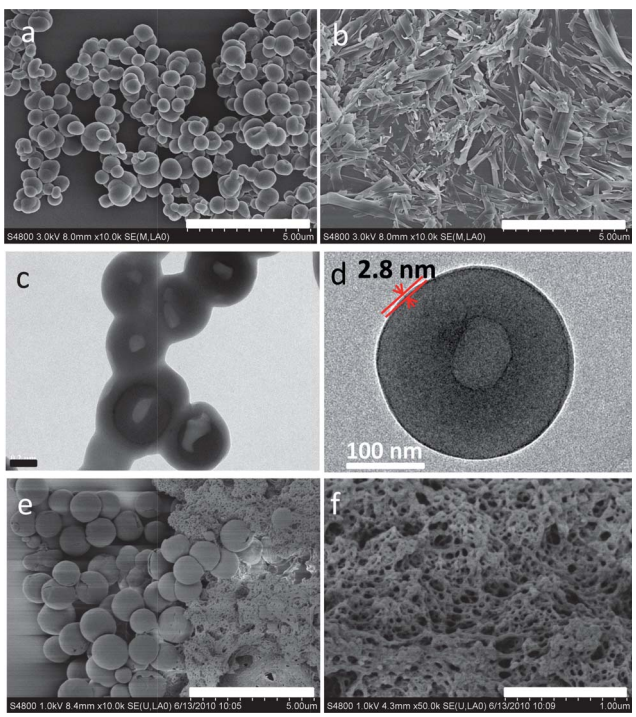

Fig. 2 SEM (a, b, e, f) and TEM (c, d) images of compound **1** from ethanol: (a, c and d) precipitate from a heating–cooling process (2.4 wt%); (b) T-gel from ethanol (4.7 wt%); (e) partial gel after sonication for 5 min (2.4 wt%); (f) S-gel after sonication for 10 min (2.4 wt%); scale bar for a, b, c, d, e and f are 5, 5, 0.2, 0.1, 5 and 1 μm, respectively.

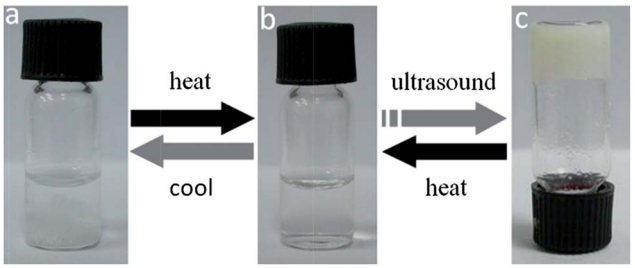

Fig. 3 Images of the exchange process between the precipitate and gel of **1** in ethanol. (a) 10 mg of **1** and 0.5 mL ethanol in a glass vial; (b) after heating at 70 °C for 15 min; (c) followed by sonication for 10 min (500 w, 40 KHz).

sample of **1** at a concentration of 2.4 wt% in ethanol was heated at 70 °C until it dissolved. As we presented, a precipitate sample at a concentration of 2.4 wt% in ethanol after the sol cooling to room temperature showed a large number of vesicles with a diameter in the range of 300–800 nm. Another transparent hot sol was placed into an ultrasonic scanner bath (500 w, 40 KHz) for 5 min to form a partial gel. The SEM image of the partial gel showed the coexistence of the vesicles with a diameter of about 1 μm and an intercrossed fiber structure; parts of the vesicles are ruptured (Fig. 2e). When the hot ethanol sol was treated with sonication for at least 10 min it completely changed into a gel (S-gel). The SEM image of the gel showed a large area of multiporous network woven by tiny fibers with a diameter of about 20–50 nm (Fig. 2f). This multiporous soft network of S-gel is different to the more highly concentrated T-gel of 4.7 wt% (Fig. 2b), which indicates the different driving force for nucleation of the aggregation between concentration and sonication. In case of the sonication, the three dimensional gel network is more highly branched and entangled.

We used a gas adsorption experiment with the BET method to determine the surface area of the solid prepared by cooling (powder, Fig. 4a) and by treatment with ultrasound (S-xerogel, Fig. 4b) with the same concentration condition of 2.4 wt%. Nitrogen adsorption/desorption isotherms indicated that the BET surface of the powder (vesicles) and the S-xerogel was about 165 $cm^2\ g^{-1}$ and 266 $cm^2\ g^{-1}$, respectively. On the basis of this data and the SEM observations, we hypothesize that the S-gel has a continuous 3D entangled network and the capillary forces within that network prevent the liquid from flowing.

Mechanical properties of the sonicated gel

The mechanical properties of the sonicated gel were studied by dynamic oscillatory measurements. The linear viscoelastic regions (LVR) of the gel were determined by strain amplitudes ranging from 0.01% to 100% at 6.28 rad s^{-1} (Fig. 5a). The strength (storage

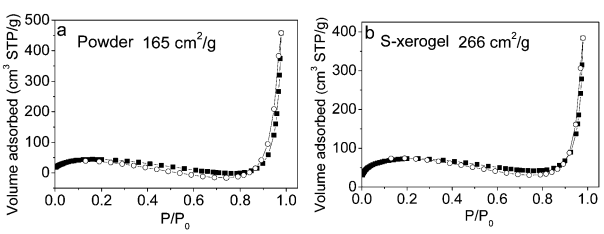

Fig. 4 N_2 sorption isotherms of (a) the powder and (b) S-xerogel.

modulus, G') of the gel is around 5000 Pa with a small strain of 0.01%. This signifies the stability of the gel towards the shearing process, which is important for the gel transportation. The storage modulus (G') and the loss modulus (G'') remain nearly constant up to approximately 0.1% strain ($G' > G''$), an outcome that defines the uppermost boundary of the LVR. This result indicates that the gel forms an inter-crossed morphology when a small strain was imposed (the linear region). Beyond this level of deformation, the gel gives a weak strain overshoot (that is, the G' value decreases, whereas the G'' value increases and then decreases) within the range of 0.1%–8%. At large strain amplitudes, the gel showed a catastrophic disruption accompanied by a steep decrease in the values of both moduli and the reversal of the viscoelastic signal ($G'' > G'$). The implementation of a frequency sweep between 0.1 and 100 rad s^{-1} shows $G' > G''$, which confirms that the gel has a predominantly elastic character (Fig. 5b). The elasticity of the gel is further evident from the fact that the G' and G'' values are minimally sensitive to frequency (w), which indicated that the gel system formed a stable network structure.[16] The double logarithmic plot of the dynamic viscosity (η^*) *versus* the angular frequency (w) has a gradient close to −1, which is characteristic of a strong cohesive gel.[17]

Structure study of the vesicles and the gel

Fourier transform infra-red (FTIR) spectra provided valuable information about the change of the molecule conformation and the intermolecular hydrogen bonding structure in the aggregate. Powder IR data shows that both the vesicles and S-xerogel had a peak at 3273 cm^{-1}, indicating the existence of hydrogen bonding in the substance (Fig. S3, see ESI†). It is important to compare the IR spectral change in the C=O stretching regions related to hydrogen bonds. Time-resolved online FTIR spectra of sol **1** over 12 mins with and without sonication, were collected in order to ascertain the molecular conformation and the formation of the ordered structure. As shown in Fig. 6, the shape of the two different C=O stretching bands, a strong band at 1658 cm^{-1} (amide group) and a medium intensity band at 1697 cm^{-1} (carbamate), were essentially unchanged with time, indicating that the conformation of **1** did not change during the cooling process. However, the spectral intensity continued to decline and the wavenumbers of the two peaks changed from 1697 and 1658 cm^{-1} to 1701 and 1650 cm^{-1}, respectively, which might be due to the enhancement of the intermolecular H-bond between amides and formation of the vesicles (Fig. 6a). By contrast, in response to the sonication, the peak at 1658 cm^{-1} corresponding to amide split into peaks at 1670 and 1650 cm^{-1},

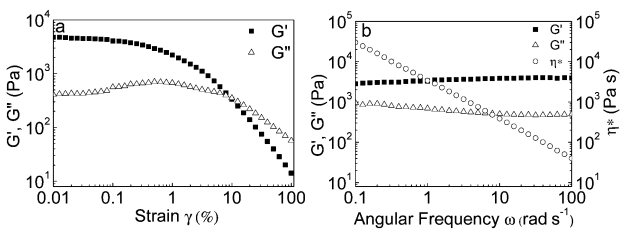

Fig. 5 Dynamic oscillatory data for the S-gel at 20 °C (2.4 wt% in ethanol); (a) strain sweep of the gel at a frequency of 6.28 rad s^{-1}; (b) frequency sweep of the gel at a strain of 0.1%.

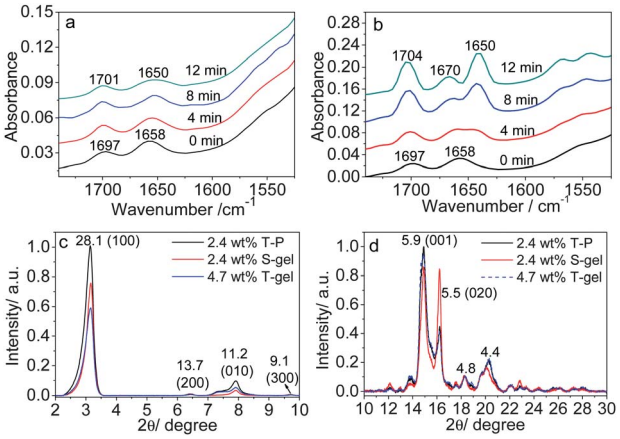

Fig. 6 Time-resolved online IR spectra of 2.4 wt% hot sol in ethanol after (a) cooling at room temperature and (b) treated with sonication at room temperature within 12 min. XRD profile of the vesicle, S-xerogel and T-xerogel of **1** in the 2θ range of (c) 1–10 ° and (d) 10–30 °.

indicating that part of the H-bonded amide was released from the aggregation due to the intermolecular interaction between ethanol and molecules of **1**. This was consistent with the increase of the stretching band intensity at both 1650 and 1704 cm^{-1} with sonication time (Fig. 6b). This might correspond to the formation of a gel network structure with a larger surface area, and more amide groups which were exposed and formed hydrogen bonds with the ethanol molecules.

The molecular packing of the vesicles and xerogel was further investigated by X-ray diffraction. The vesicles, S-xerogel and T-xerogel have similar X-ray diffraction profiles; all show a series of peaks corresponding to distances of 28.0 Å, 13.8 Å and 9.1 Å, with a ratio of 1 : 1/2 : 1/3, indicating a lamellar packing of the molecules (Fig. 6c, 6d). The distance of 28.0 Å was close to the length of the molecule of **1** (Fig. S4, see ESI†), suggesting that the molecules aggregated as a parallel structure by intermolecular hydrogen bonding between the imide (C=O) and amide (N–H) (as shown by the IR data), hydrophobic interaction of the adamantane and cholesterol groups. Through the computer mimic of molecule **1**, we know that the width of the cholesterol group was about 5.5 Å and the width of adamantine group was about 5.1 Å. The peak at 11.2 Å is just about twice the width of a cholesterol group (5.5 Å), which may represent the distance between the hydrophobic groups. This difference of the width between the cholesterol and adamantane group (0.4 Å) may lead to curving of the lamella, and thus form a single layer vesicle with a thickness of 2.8 nm and a diameter of 200–800 nm (Fig. 7). With the sonication irradiation, the pattern of X-ray diffraction has no change, only the comparative intensity of the peaks between 5.5 Å and 5.9 Å obviously increases. This may lead to the different nucleation direction of the aggregation between vesicles and the S-gel. This result is different to our previous report[13] and other published results[18] in which the conformation of the molecules or the symmetry of coordination polyhedron was slightly tuned by the sonication irradiation with the change of morphology.

On the basis of the data presented above, we hypothesise that the molecule **1** is arranged irregularly in the hot transparent

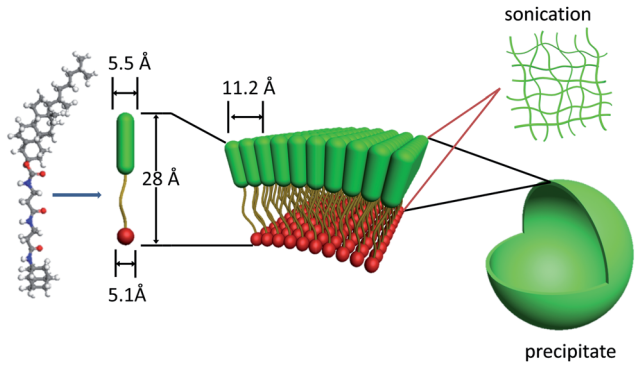

Fig. 7 Schematic representation of aggregation changes of **1** in cooling and sonication process.

ethanol solution. The irregular molecules are self-assembled as a lamellar structure by intermolecular hydrogen bonding and hydrophobic interactions in the cooling process. One lamella is formed as shown in Fig. 7. Finally, the molecules are self-assembled into shells that accumulate and precipitate. When the ethanol solution is placed into the ultrasonic scanner, the ultrasound generated cavitation effect resulted in temporary destruction of the aggregate and the dissolution of small quantities of molecules, disturbing the long range arrangement of the layer into vesicles.[10] Thus, the layers are rapidly twisted and enwound under nonequilibrium conditions and instantaneously form a fibrous material without time for full crystallization to take place.[12] This entangled 3D fibrous structure has greater porosity than that of a vesicle structure and can accommodate many more ethanol molecules in the formation of a gel.

Conclusions

In conclusion, we have designed and synthesized a novel kind of low weight molecular gelator that could be self-assembled into vesicles and a three dimensional nano network in ethanol by a heating–cooling and a heating–sonication process, respectively. The morphology can also be changed from vesicles to ribbons by increasing the concentration of the molecules. On the basis of online IR spectra, the SEM and rheology studies, we propose that during the exchange the gelator molecules are arranged as lamella structures by intermolecular hydrogen bonding and hydrophobic interactions. The lamella further self-assemble to a vesicle structure in the heating–cooling process. The effect of ultrasound is to disturb the long arrangement of the lamella by inserting the ethanol molecules into the self-assembly of gelators and form a three dimensional network so that the ethanol solution is changed into a gel. The exchange of morphology between vesicles and a gel network through a supramolecular self-assembly effect in response to ultrasound and heating may be useful for the applications of these soft materials in areas such as responsive materials or shape-memory materials, storage, absorption and delivery systems, which we are currently exploring as some of the possibilities.

Acknowledgements

This work was supported by the National Science Foundation of China (91022021 and 21125104), National Basic Research Program of China (2009CB930400), Program for Innovative Research Team in University (IRT1117), and Shanghai Leading Academic Discipline Project (B108).

Notes and references

1 R. P. Sijbesma, F. H. Beijer, L. Brunsveld, B. J. B. Folmer, J. H. K. Hirschberg, R. F. M. Lange, J. K. L. Lowe and E. W. Meijer, *Science*, 1997, **278**, 1601; A. Schenning and E. W. Meijer, *Chem. Commun.*, 2005, 3245; P. Cordier, F. Tournilhac, C. S. Ziakovic and L. Leibler, *Nature*, 2008, **451**, 977; Y. Lin, A. Boker, J. B. He, K. Sill, H. Q. Xiang, C. Abetz, X. F. Li, J. Wang, T. Emrick, S. Long, Q. Wang, A. Balazs and T. P. Russell, *Nature*, 2005, **434**, 55; J. T. Davis and G. P. Spada, *Chem. Soc. Rev.*, 2007, **36**, 296; P. A. Monnard and D. W. Deamer, *Anat. Rec.*, 2002, **268**, 196.

2 H. Yan, S. H. Park, G. Finkelstein, J. H. Reif and T. H. LaBean, *Science*, 2003, **301**, 1882; J. M. Lehn, *Chem. Soc. Rev.*, 2007, **36**, 151; I. W. Hamley, *Nanotechnology*, 2003, **14**, R39; C. F. J. Faul and M. Antonietti, *Adv. Mater.*, 2003, **15**, 673; J. Y. Cheng, A. M. Mayes and C. A. Ross, *Nat. Mater.*, 2004, **3**, 823; X. F. Zhu, P. F. Duan, L. Zhang and M. H. Liu, *Chem.–Eur. J.*, 2011, **17**, 3429.

3 Y. Bae, S. Fukushima, A. Harada and K. Kataoka, *Angew. Chem., Int. Ed.*, 2003, **42**, 4640.

4 F. Caruso, *Chem.–Eur. J.*, 2000, **6**, 413; D. H. W. Hubert, M. Jung and A. L. German, *Adv. Mater.*, 2000, **12**, 1291; J. Liu, S. B. Hartono, Y. G. Jin, Z. Li, G. Q. Lu and S. Z. Qiao, *J. Mater. Chem.*, 2010, **20**, 4595.

5 S. Jain and F. S. Bates, *Science*, 2003, **300**, 460; Y. Wang, H. Xu and X. Zhang, *Adv. Mater.*, 2009, **21**, 2849; M. Antonietti and S. Forster, *Adv. Mater.*, 2003, **15**, 1323; D. Lingwood and K. Simons, *Science*, 2010, **327**, 46.

6 A. Ajayaghosh, R. Varghese, S. Mahesh and V. K. Praveen, *Angew. Chem., Int. Ed.*, 2006, **45**, 7729; D. Ke, C. Zhan, A. D. Q. Li and J. Yao, *Angew. Chem., Int. Ed.*, 2010, **50**, 3715; Q. Wang, J. Wu, Z. Gong, Y. Zou, T. Yi and C. Huang, *Soft Matter*, 2010, **6**, 2679.

7 J. H. Jung, Y. Ono, K. Sakurai, M. Sano and S. Shinkai, *J. Am. Chem. Soc.*, 2000, **122**, 8648; M. Numata and S. Shinkai, *Chem. Commun.*, 2011, **47**, 1961; M. Numata, K. Kaneko, H. Tamiaki and S. Shinkai, *Chem.–Eur. J.*, 2009, **15**, 12338.

8 W. Cai, G. T. Wang, Y. X. Xu, X. K. Jiang and Z. T. Li, *J. Am. Chem. Soc.*, 2008, **130**, 6936; Y. X. Xu, G. T. Wang, X. Zhao, X. K. Jiang and Z. T. Li, *Langmuir*, 2009, **25**, 2684.

9 T. Naota and H. Koori, *J. Am. Chem. Soc.*, 2005, **127**, 9324; C. Wang, D. Q. Zhang and D. B. Zhu, *J. Am. Chem. Soc.*, 2005, **127**, 16372; R. Wang, X. Liu and J. Li, *Cryst. Growth Des.*, 2009, **9**, 3286.

10 G. Cravotto and P. Cintas, *Chem. Soc. Rev.*, 2009, **38**, 2684; D. Bardelang, *Soft Matter*, 2009, **5**, 1969.

11 N. Komiya, T. Muraoka, M. Iida, M. Miyanaga, K. Takahashi and T. Naota, *J. Am. Chem. Soc.*, 2011, **133**, 16054; J. M. J. Paulusse and R. P. Sijbesma, *Angew. Chem., Int. Ed.*, 2006, **45**, 2334; J. M. J. Paulusse, D. J. M. van Beek and R. P. Sijbesma, *J. Am. Chem. Soc.*, 2007, **129**, 2392.

12 X. Yu, Q. Liu, J. Wu, M. Zhang, X. Cao, S. Zhang, Q. Wang, L. Chen and T. Yi, *Chem.–Eur. J.*, 2010, **16**, 9099.

13 J. Wu, T. Yi, T. Shu, M. Yu, Z. Zhou, M. Xu, Y. Zhou, H. Zhang, J. Han, F. Li and C. Huang, *Angew. Chem., Int. Ed.*, 2008, **47**, 1063; J. Wu, T. Yi, Q. Xia, Y. Zou, F. Liu, H. Dong, T. Shu, F. Li and C. Huang, *Chem.–Eur. J.*, 2009, **15**, 6234.

14 M. Zhang, S. Sun, X. Yu, X. Cao, Y. Zou and T. Yi, *Chem. Commun.*, 2010, **46**, 3553.

15 J.-L. Li, B. Yuan, X.-Y. Liu and H.-Y. Xu, *Cryst. Growth Des.*, 2010, **10**, 2699.

16 F. M. Menger and K. L. Caran, *J. Am. Chem. Soc.*, 2000, **122**, 11679; K. hyun, S. H. Kim, k. H. Ahn and S. J. Lee, *J. Non-Newtonian Fluid Mech.*, 2002, **107**, 51; K. Hyun, J. G. Nam, M. Wilhellm, K. H. Ahn and S. J. Lee, *Rheol. Acta*, 2006, **45**, 239.

17 S. Kasapis, I. M. Al-Marhoobi, M. Deszczynski, J. R. Mitchell and R. Abeysekera, *Biomacromolecules*, 2003, **4**, 1142; S. Srinivasan, S. S. Babu, V. K. Praveen and A. Ajayaghosh, *Angew. Chem., Int. Ed.*, 2008, **47**, 5746; S. Yao, U. Biginn, T. Gress, M. Lysetska and F. Würthner, *J. Am. Chem. Soc.*, 2004, **126**, 8336.

18 S. Zhang, S. Yan, J. Lan, Y. Tang, Y. Xue and J. You, *J. Am. Chem. Soc.*, 2009, **131**, 1689.

